Journal of Molecular Liquids 385 (2023) 122379

Contents lists available at ScienceDirect

Journal of Molecular Liquids

journal homepage: www.elsevier.com/locate/molliq

Electrically induced transformation of cholesteric droplets under homeotropic boundary conditions

Mikhail N. Krakhalev [a,b,*], Anna P. Gardymova [a,b], Vladimir Yu. Rudyak [c], Vadim A. Barbashov [d], Victor Ya. Zyryanov [a]

[a] Kirensky Institute of Physics, Federal Research Center KSC SB RAS, 50/38 Akademgorodok, Krasnoyarsk, 330036, Krasnoyarsk region, Russia
[b] Institute of Engineering Physics and Radio Electronics, Siberian Federal University, 79 Svobodny Pr., Krasnoyarsk, 660041, Krasnoyarsk region, Russia
[c] Faculty of Physics, Moscow State University, 1/2 Leninskiye Gory, Moscow, 119991, Moscow, Russia
[d] P.N. Lebedev Physical Institute of the Russian Academy of Sciences, 53 Leninsky Pr., Moscow, 119991, Moscow, Russia

ARTICLE INFO

Keywords:
Cholesteric droplet
Orientational structure
Topological defect
Electric field
Structure relaxation

ABSTRACT

Cholesteric droplets under homeotropic boundary conditions demonstrate a rich variety of possible orientational structures. We have implemented electrically controlled switching of such droplets between two classes of stable states: *i*) structures with cylindrical cholesteric layers and *ii*) layer-like structures with one or more $\lambda^{+1/2}$-disclinations. Structure relaxation after switching off the voltage proceeded via the fast (less than 1 s), the slow (more than 1 s), and the stabilization stages (~ 10 hours). We investigated intermediate long-lived metastable states occurring in the relaxation process and explained the formation of various structures in cholesteric droplets. The fast and the slow stages of relaxation were found to be sensitive to the voltage reduction regime. We have determined the combinations of droplet size and voltage reduction regimes leading to the two types of structures after relaxation.

1. Introduction

Liquid crystals are essentially anisotropic molecular liquids characterized by rich and complex physics [1]. The droplet dispersions of the liquid crystals (LCs) have unique optical properties, particularly in the case of cholesteric LC (CLCs) [2]. It is widely used in electro-, thermo-, chemo- or mechanically programmed lasers [3–7], smart films [8–11], chemo- and biosensors [12–16], anti-counterfeiting material [17], and in other novel approaches and applications [18–21].

Optical properties of CLC droplets are determined by the formed orientational structure, which depends in a complicated way on the boundary conditions, material parameters of the CLC, and the size of the droplet (characterized by the ratio of the droplet diameter d to the cholesteric intrinsic helix pitch p_0, so-called relative chiral parameter $N_0 = 2d/p_0$ [22]).

A rich variety of different director configurations can form in the droplets of cholesteric under homeotropic boundary conditions [23–25]. It allows to obtain cholesteric droplets with different topological states and implement switching between them. For example, metastable structures with a different number of bulk point defects can occur upon quickly cooling of a CLC from an isotropic phase [26,27]. At the same time, transitions between different metastable CLC structures have been less studied. In particular, an electrically controlled switching from a twisted radial structure to a twisted toroidal configuration [28], intermediate stable structures [29] or between a structure with a bipolar distribution of the helix axis and a structure with $\lambda^{+1/2}$- or $\lambda^{-1/2}$-disclination [30] were implemented.

Thus, further progress towards the practical use of this knowledge requires the ability to switching between various states of droplets in a film.

In this paper, we explored the possibility of switching CLC droplets with homeotropic boundary between different stable and metastable structures. We studied experimentally the response of such droplets to the applied electric field. The dynamics and features of the relaxation process in droplets of various chiral parameter N_0 under different switching regimes were examined. Finally, we demonstrated how the cylindrical layer structure can be switched to layer-like structure, lo-

* Corresponding author at: Kirensky Institute of Physics, Federal Research Center KSC SB RAS, 50/38 Akademgorodok, Krasnoyarsk, 330036, Krasnoyarsk region, Russia.
E-mail address: kmn@iph.krasn.ru (M.N. Krakhalev).

https://doi.org/10.1016/j.molliq.2023.122379
Received 19 January 2023; Received in revised form 13 June 2023; Accepted 15 June 2023
Available online 22 June 2023

cally similar to the cholesteric ground state [31], and backwards in an easy, robust, and reproducible way.

2. Materials and methods

Polymer dispersed liquid crystal (PDLC) films based on poly(isobutyl methacrylate) (PiBMA) (Sigma Aldrich) and the nematic E7 (Synthon) doped with cholesteryl acetate (Sigma Aldrich) were used. CLCs with the intrinsic helix pitches $p_0 = 5.5$ μm and $p_0 = 4.1$ μm were studied. PDLC films with CLC droplets with the relative chiral parameter of $6.0 < N_0 < 15.0$ (the droplet size measured in the PDLC plane was used at calculating N_0) were obtained by combined phase separation technology [28]. CLC droplets had spheriod shape with the oblateness degree (the ratio between the minor and the major axes) not lower than 0.6 (see Fig. 5 inset in [28] for details). The electric field was applied perpendicular (first type of PDLC cells) or parallel (second type of PDLC cells) to the PDLC film plane, same as in ref. [32]. In the first type cells, two identical ITO coated glass substrates were used. For the second type, two ITO electrodes separated by $H \cong 100$ μm gap were on the one substrate, and the second glass substrate was without electrodes. The investigated PDLC film was placed between the substrates, 20 μm diameter glass microspheres (Duke Scientific Corporation) set composite film thickness. AC electric field with 1 kHz frequency and various magnitudes was applied to PDLC cells. A polarizing optical microscope (POM) Axio Imager.M1m (Carl Zeiss) was used to study the orientational structures of CLC droplets and their response to an electric field. The orientation and shape of the cholesteric layers formed in CLC droplets were determined from the location of the isoclinic lines observed in the optical texture, as described in Ref. [33] in detail. The location of the isoclinic lines corresponds to the areas at the focal plane where the director is oriented along the optical axis of the microscope (perpendicular to the PDLC film). Using PDLC cells of the two types makes it possible to observe the location of cholesteric layers in the droplet's cross-sections oriented perpendicularly and parallel to the applied electric field, respectively.

3. Results and discussion

Initially, we observe the layer-like structure with bipolar distribution of the cholesteric helix axis in CLC droplets of PDLC film. Under gradually increasing electric field, three characteristic changes in the droplet structure occur consequently [33]. First, bipolar axes in all droplets become oriented perpendicular to the applied field. Then cholesteric helices unwind gradually, and the number of cholesteric layers decreases. As a result, a few narrow regions of 180°-turn of the director are formed in the droplets. Finally, the further increase of electric field leads to the discrete decreasing the cholesteric layers number up to their complete disappearance. After that, the droplet structure features the circular defect located at the equator of the droplet and oriented perpendicular to an electric field. This circular defect is kept in the structure in the electric fields $E \geq 3.0$ V/μm (see Supplementary Figure S1). An increase in the voltage leads to an increasing the droplet' central region with the uniform director orientation and reducing the thickness of the LC layer near the circular defect, where the director is the 90°-twisted [28].

We started from this configuration and investigated the droplets reaction to the decreasing electric field. Similar to the case of the cholesteric droplets abruptly cooled from an isotropic state [31], the relaxation process under decreasing voltage consists of several stages. *The fast stage* passes in the first tenths of a second, when the initial toron structure twists and forms cholesteric layers in various ways. *The fast stage* dynamics is primarily determined by the viscosity and the elasticity constants of the CLC, the helix pitch p_0, and the droplet's size [34]. Then movement and transformation of the topological defects occurs during *the slow stage*, which results in the formation of a metastable configuration that remains practically unchanged for several

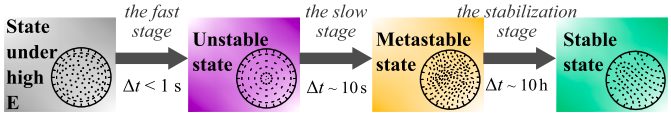

Fig. 1. The sequence of structural states of CLC droplets and the dynamics of transitions between them. In the lower right corner there are schemes of the director (dashed and dotted lines) configuration in the equatorial cross-section of droplet for the unwinded toron structure (State under high E), the twisted toron configuration (Unstable state), the layer-like structure with several $\lambda^{+1/2}$-disclinations (Metastable state), and the layer-like structure with one $\lambda^{+1/2}$-disclination (Stable state).

hours or tens of hours. *The slow stage* dynamics depends primarily on the features of surface anchoring and can pass for several tens of seconds [35]. Finally, during *the stabilization stage* the metastable configuration transforms into a stable one (Fig. 1). This stage is characterized by a decrease in the bending of cholesteric layers (for example, a decrease in the $\lambda^{+1/2}$-disclinations number). It typically passes for several hours [36]. The dynamics of this stage depend primarily on the N_0 value and the height of the energy barrier (symmetry) of the formed metastable structure.

We decreased electric field in two regimes: step-wise decrease (each change of the value of E is less than 0.5 V/μm) and rapid switch off (E value change is over 1.0 V/μm). We found that the dynamics of structure relaxation and the final state strongly depends on the regime of decrease, as well as on the magnitude of the applied field from which the voltage is switched off and the N_0 value. Depending on these factors, two key mechanisms for the cholesteric layers formation can be realized: curving of the circular defect or the appearance of the director twist in the bulk.

3.1. Curving of the circular defect

First, we studied step-wise decrease of the electric field. For this, we decreased the electric field by 0.1 V/μm above the transition threshold (0.3 V/μm). At 0.4 V/μm and above, the droplets remain in toron configuration (Fig. 2a). At 0.3 V/μm, the structural changes occur. During the first stage, the droplet structure shows almost no changes (Fig. 2a,b). The director is the 90°-twisted near the circular defect. In the slow stage, the twist angle grows in a small area near the droplet surface and is accompanied by a S-shaped curvature of the circular defect (Fig. 2c,d, Supplementary Movie 1). Further, the director 180° twist gradually occupies a substantial volume of the droplet and forms a stable CLC configuration with $\lambda^{+1/2}$-disclination (Fig. 2e-f). In the optical texture, the formation of the $\lambda^{+1/2}$-disclination corresponds to the appearance of two lines, where the director is oriented perpendicular to the PDLC film plane (Fig. 2e,f) [33]. Then, additional cholesteric layers are formed (lines in the droplet optical texture in Fig. 2g), which number depends on the value of N_0 [30]. Finally, there are almost no changes in this droplet layer-like structure during the stabilization stage (Fig. 2h).

3.2. Appearance of the director twist in the bulk

The appearance of $\lambda^{+1/2}$-disclination shown above is a slow process. The structural changes can proceed in another way and the formation of cholesteric layers starts from the droplet' bulk. In particular, such relaxation occurs when the electric field is abruptly switched off. In this regime, the director near the surface circular defect does not have time to form a cholesteric layer. Instead, during the fast stage the central (bulk) part of the droplet twists, and the resulting director configuration depends on the N_0 value and the magnitude of the electric field before switching off (Fig. 3a,b).

In larger droplets with $N_0 > 8.0$, the axisymmetric structure is formed in case of the electric field before switch off $E > 1.5$ V/μm (Fig. 3b (top row), Supplementary Figure S2). Two pairs of isoclinic

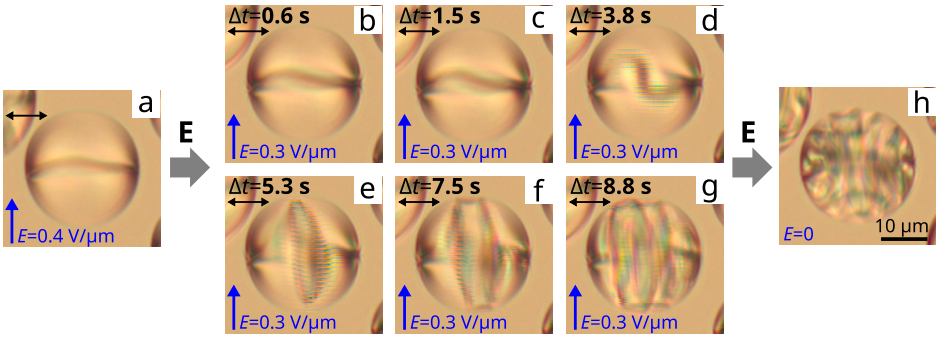

Fig. 2. POM photos of the CLC droplet at $N_0 = 9.1$ (taken from Supplementary Movie 1) under the action of the electric field $E = 0.40$ V/μm (a), taken in $\Delta t = 0.6$ s (b), 1.5 s (c), 3.8 s (d), 5.3 s (e), 7.5 s (f) and 8.8 s (g) after decreasing E to 0.3 V/μm, and after switching off the voltage (h). Hereinafter, the blue arrow shows the direction of the electric field applied along PDLC film plane, and the black double arrow indicates the polarizer orientation.

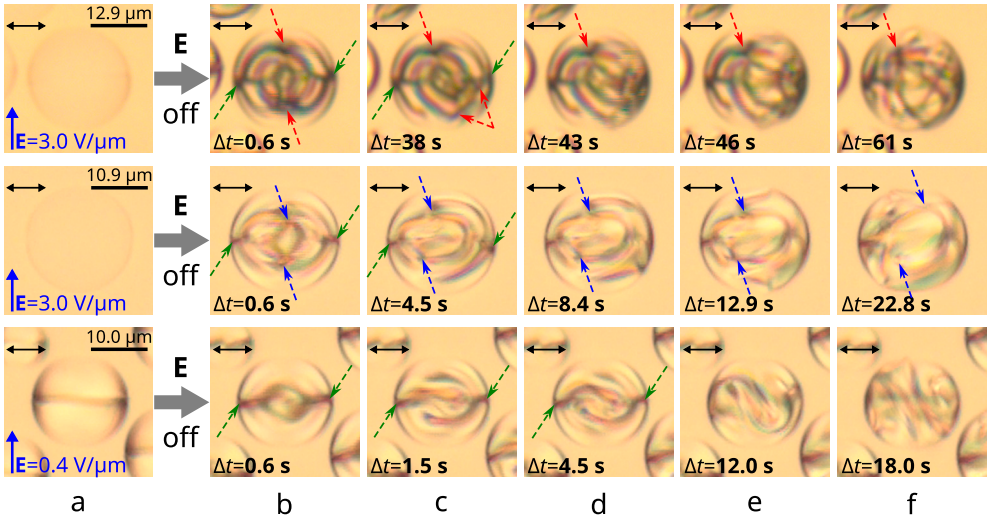

Fig. 3. POM photos of the cholesteric droplets at $N_0 = 8.4$ (top row, taken from Supplementary Movie 2), $N_0 = 7.6$ (middle row, taken from Supplementary Movie 3), and $N_0 = 6.4$ (bottom row, taken from Supplementary Movie 4). CLC droplets under the action of an electric field (a) and in Δt seconds after the voltage is turned-off (b)-(f). The applied electric field strength E and the corresponding time Δt are indicated in photos. The applied electric field is parallel to the PDLC film plane. Red and blue dotted arrows show the bulk defects positions with topological charge $|m| = 2$ and $|m| = 1$, respectively. Green dotted arrows show the cross-sections of the surface circular defect.

lines are visible in the optical texture of CLC droplet, which corresponds to two pairs of cholesteric layers joining in two sites (shown by red dotted arrows in Fig. 3) located on the structure symmetry axis. In one site, the isocline lines join to a point (point defect) (shown by the upper dotted red arrow), while in the lower part of the droplet, the joining of cholesteric layers occurs in a small area (ring defect) (shown by the lower dotted red arrow). Each pair of closed cholesteric layers has two topological defects with $|m| = 1$ [26], so the structure with two enclosed cholesteric layers with point and ring defects with topological charges $|m| = 2$ are formed after abruptly turning off the voltage. The formation of enclosed cholesteric layers does not change the position of the surface circular defect (indicated by the green dotted arrows in Fig. 3). These enclosed layers correspond to 4 cholesteric layers along the droplet diameter. Near the surface circular twist-defect, the director additionally twists by $\pi/2$. Thus, after turning off voltage, a structure with 5 cholesteric layers is formed, which is less than the number of layers in CLC droplets with the bipolar distribution of the helix axis at $N_0 > 8.0$ [37]. Such an unwinded cholesteric state is not stable, and the structure is gradually transformed into a layer-like structure later during the slow stage (Fig. 3b-f (top row)). This transformation begins with the interaction and merges of surface and bulk ring defect, followed by the opening of the cholesteric layers (Fig. 3b-e (top row), Supplementary Movie 2). This stage of structure change takes several tens of seconds and proceeds without the destruction or transformation of the bulk point defect (Fig. 3f, top row). The resulting structure is metastable and persists from several hours to several days. Finally, during the stabilization stage the point defect breaks and the layer-like configuration (with $\lambda^{+1/2}$-disclination or with bipolar distribution of the cholesteric axis) establishes.

In smaller droplets with $6.0 < N_0 < 8.0$, only one enclosed cholesteric layer and a pair of the point defects of topological charge $|m| = 1$ is formed during the fast stage in the central part of the droplet (Fig. 3b (middle row), Supplementary Figure S3). The electric field before switching off should be not less than 1.5 V/μm. The number of cholesteric layers in this structure is about 3, which makes it unstable. The symmetry of the formed configuration is broken within a few seconds (Fig. 3c (middle row), Supplementary Movie 3) during the slow stage. Consequently, the surface circular defect curves (Fig. 3d,e, middle row), and a metastable structure with a pair of point defects is formed (Fig. 3f, middle row). Finally, within several hours of the stabilization stage, this metastable structure transforms into a structure with $\lambda^{+1/2}$-disclination.

The formation of a cholesteric layer from the droplet' bulk can be also occurred at step-wise decrease of the electric field. In this case, when the applied field is switched off from $E < 1.0$ V/μm, the twisted toroidal configuration remains in the droplet for several tenths of a second after switching off an electric field (Fig. 3a,b, bottom row). Then, the director additionally twists in the droplet center and CLC config-

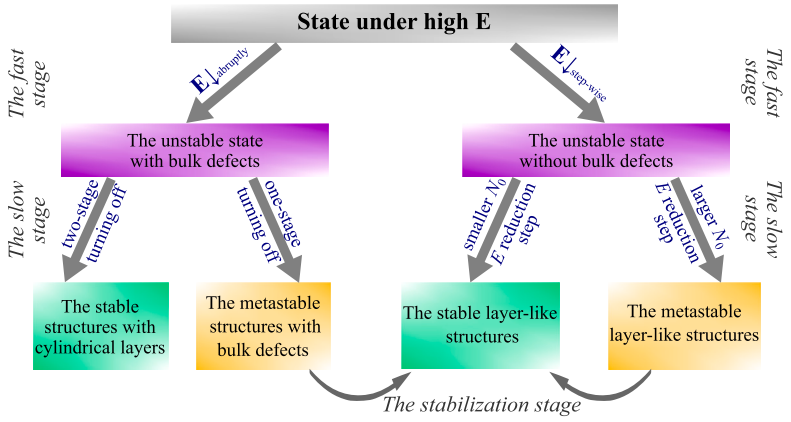

Fig. 4. Scheme of both realized transitions and parameters controlling the relaxation process of CLC droplet structures under homeotropic anchoring.

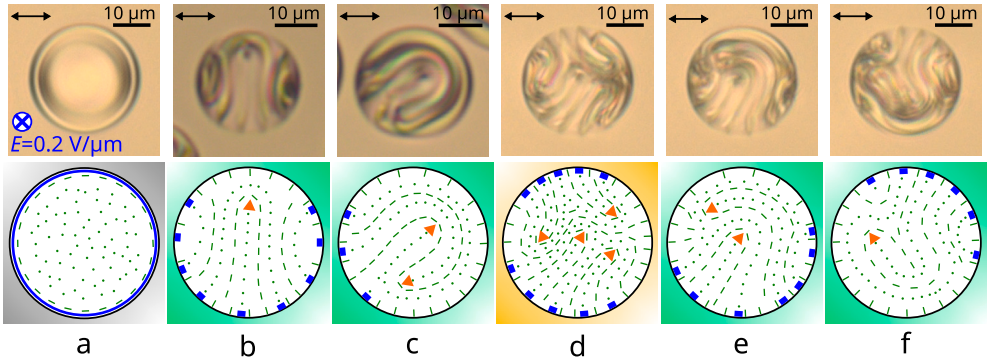

Fig. 5. POM photos of the cholesteric droplet at $N_0 = 10.9$ under the action of the electric field applied perpendicular to the PDLC film (a), and CLC droplets at $N_0 = 9.1$ (b), $N_0 = 10.0$ (c) and $N_0 = 10.9$ (taken from Supplementary Movie 5 – Movie 7) (d)–(f) after switching off voltage (top row). Corresponding schemes of the director (dashed and dotted lines) configuration in the equatorial cross-section of droplets (bottom row). The circular equatorial twist defect is shown by the blue ring. Hereinafter, the cross-sections of twist linear defect and $\lambda^{+1/2}$-disclinations are indicated by the blue rectangles and orange triangles, respectively. The background color on the director configuration schemes corresponds to the structure stability in accordance with Fig. 1: grey - state under high **E**, magenta - unstable state, yellow - metastable state, and green - stable state.

uration transforms gradually into the structure with $\lambda^{+1/2}$-disclination during the slow stage (Fig. 3c-h (bottom row), Supplementary Movie 4). There is no further evolution in the structure, and this layer-like structure remains unchanged in the stabilization stage. We analyzed this transition in more detail in ref. [30].

3.3. Switching between different topological states of CLC droplets

The demonstrated scenarios of structure relaxation are determined solely be the regime of electric field turning off in a wide range of droplet sizes. Thus the structure relaxation can be controlled both at the fast stage and at the slow stage, and the desired stable state can be obtained. It allows one to easily and reproducibly switch the droplet between different states. For this, high electric field should be applied, and then the desired topological state can be reached by implementing a corresponding relaxation scenario (Fig. 4).

By choosing the electric field regime various metastable structures can be obtained, that remain unchanged for several hours. These metastable structures transform into the next metastable states when the electric field is decreased below $E < 0.40$ V/μm. In the case of metastable configurations with bulk defects, such structure changes consist in the reorientation of cholesteric layers without the transformation of bulk defects. Transformation and/or annihilation of bulk defects occurs in strong fields, almost completely unwinding the CLC structure.

Next, we consider several types of the forming complex CLC structures, as well as a number of examples of the switching of cholesteric droplets between various topological states.

3.3.1. CLC structures with several $\lambda^{+1/2}$-disclinations

During relaxation from the unwinded toron state (Fig. 5a) structures with $\lambda^{+1/2}$-disclination are formed in CLC droplets at $N_0 > 6.0$. Since the cholesteric layer with $\lambda^{+1/2}$-disclination has approximately two π-turns of the director, an additional twisting of the director should occur in the droplets. For example, two additional cholesteric layers are formed in the droplets (Fig. 5b) [30]. Another possible scenario is an additional bending of the cholesteric layer with $\lambda^{+1/2}$-disclination, which occurs during the structure relaxation. As a result, only one cholesteric layer fills the whole bulk of the droplet, which prevents the formation of another cholesteric layers (Fig. 5c).

The circular defect curving may occur simultaneously at different parts of the droplet equator, which leads to the formation of the cholesteric layer with $\lambda^{+1/2}$-disclination (Fig. 2d,e). As a result, several $\lambda^{+1/2}$-disclinations may appear in the droplets, the number of which is limited by the number of cholesteric pitches. For instance, the structure with four $\lambda^{+1/2}$-disclinations is formed in CLC droplet at $N_0 = 10.9$ when the electric field decreases from $E = 0.2$ V/μm to $E = 0.15$ V/μm (Fig. 5d, Supplementary Movie 5). The protocol of decreasing the applied electric field will affect the relaxation and type formed CLC structure. As an example, Fig. 5d-f shows the same CLC droplet at different orientational states. When the electric field is switched from $E = 0.25$ V/μm to $E = 0.15$ V/μm, two cholesteric layers with $\lambda^{+1/2}$-disclination emerge at first and fill the whole bulk of the droplet (Supplementary Movie 6). It suppresses the formation of more cholesteric layers, and the structure with two $\lambda^{+1/2}$-disclinations occurs (Fig. 5e). If the electric field is switched from $E = 0.25$ V/μm to $E = 0.18$ V/μm, the only one bent cholesteric layer with $\lambda^{+1/2}$-disclination is formed,

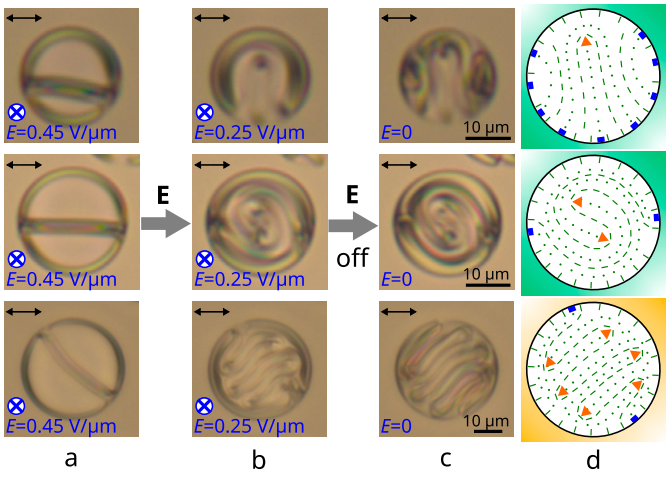

Fig. 6. POM photos of the cholesteric droplets at $N_0 = 8.0$ (top row), $N_0 = 9.0$ (middle row) and $N_0 = 13.5$ (bottom row). CLC droplets are under the action of the electric field $E = 0.45$ V/μm (a), $E = 0.25$ V/μm (b), and after switching off voltage (c). Corresponding schemes of the director configuration in the equatorial cross-section of droplets (d).

filling almost the whole volume of the droplet (Fig. 5f, Supplementary Movie 7).

Bending of the cholesteric layer during structure relaxation can occur in an incompletely unwinded structure with the remaining one cholesteric layer (Fig. 6a). In that case, a step-wise decrease of the electric field leads to the bending of the cholesteric layer and the subsequent the appearance of one, two or more $\lambda^{+1/2}$-disclinations (Fig. 6b-d), depending on the value of N_0. The structure with a pair of $\lambda^{+1/2}$-disclinations located near the droplet center (Fig. 6 (middle row)) is stable. Structures with several $\lambda^{+1/2}$-disclinations are less stable and in most such droplets relax into a structure with one or two $\lambda^{+1/2}$-disclinations during twenty four hours.

3.3.2. CLC structures with cylindrical cholesteric layers

As mentioned before, the structure with two enclosed cholesteric layers is unstable (see Fig. 3, top row and Fig. 7a,b). A small electric field $0.10 < E < 0.35$ V/μm applied to this structure leads to aligning of the cholesteric layers along the field direction and shifting the ring and point defect to the opposite poles of the droplet (Fig. 7c, Supplementary Movie 8). Finally, the defects come close to the droplet boundary, and two cholesteric layers form cylinders (Fig. 7d). The new structure with the two cylindrical cholesteric layers is stable and persists after turning off the electric field (Fig. 7e,f).

The formation of enclosed cholesteric layers (Fig. 7b) corresponds to the fast stage of the structure relaxation, and the process of cholesteric layers alignment under the action of a small electric field (Fig. 7c,d) can be attributed to the slow stage of the structure relaxation. Thus it is possible to use the two-stage switching off of the electric field to switch the CLC droplet into a stable structure with the double cylindrical cholesteric layers (Fig. 7e,f). To do this, the applied electric field $E > 1.5$ V/μm should be abruptly reduced to a small stabilizing value $0.10 < E < 0.35$ V/μm, followed by its switching off after a few seconds. The structure with the double cylindrical cholesteric layers obtained in this way is stable in CLC droplets at $8.0 < N_0 < 10.0$.

A structure with one cylindrical cholesteric layer is formed during two-stage switching off of the electric field in CLC droplets at $6.0 < N_0 < 8.0$ (Fig. 8a-d, Supplementary Movie 9). In contrast to the structure with the double cylindrical cholesteric layers, this structure is unstable if the small electric field is turned-off. The formation of additional twisting of the director at the droplet periphery can stabilize this structure similar to the case of the structure with the one $\lambda^{+1/2}$-disclination (see Fig. 5b). For example, maintaining the small field $E = 0.1$ V/μm for several tens of seconds leads to the formation of an additional cholesteric layer to the left and right of the center of CLC droplet at $N_0 = 7.9$ (Fig. 8e-g). As a result, the number of the director π-turns along droplet diameter increases and the new structure is stable after the voltage is turned-off (Fig. 8h,i).

3.3.3. Combined CLC structures

Furthermore, the various elements of cholesteric structures discussed above (Figs. 5–8) can be implemented simultaneously in a single droplet, forming a *combined* director configuration. For this, large droplets ($N_0 > 9.0$) should be taken, and the regime of electric field decrease should be specifically adjusted. We show below a few typical examples.

First, when droplet relaxes from the incompletely unwinded configuration (Fig. 6a), a cholesteric layer with $\lambda^{+1/2}$-disclination appears on the droplet boundary. For the droplets shown in Fig. 9a,b, it occurs when the electric field decreases from $E = 0.45$ V/μm to $E = 0.20$ V/μm. Consequently, it leads to either bend of the existing cholesteric layer (Fig. 9a), or distortion of the structure with the pair of $\lambda^{+1/2}$-disclinations in the droplet center (Fig. 9b). After this, the electric field can be switched off, and the resulting structures will remain.

Second, in the incompletely unwinded structure at $N_0 = 12.9$, enclosed cholesteric layers appear when the electric field $E = 1.5$ V/μm is turned off abruptly. As a result, a configuration with connected three cholesteric layers is formed (Fig. 9c).

In the third case, the electric field is switched off in the following way. First, the field is abruptly switched from large value (completely unwinded structure) to a low stabilizing field. The resulting structure has two cylindrical cholesteric layers. Then after initial structure transformation, the electric field is gradually decreased to zero, which leads to the formation of cholesteric layers with $\lambda^{+1/2}$-disclination along the droplet equator. The number of $\lambda^{+1/2}$-disclinations increases with N_0 (Fig. 9d,e). For the droplets shown in Fig. 9d,e, it occurs when the electric field decreases from $E = 2.5$ V/μm to $E = 0.5$ V/μm and followed by voltage reduction to zero.

4. Conclusion

In this work, we studied the relaxation of CLC droplet structure in different regimes of decreasing electric field. Droplets with charactaristic size parameter $6.0 < N_0 < 15.0$ were studied. We distinguished the three stages of structure relaxation: *the fast stage* ($\Delta t < 1$ s), *the slow stage* ($\Delta t \sim 10$ s), and *the stabilization stage* ($\Delta t \sim 10$ h). The fast and slow stages of relaxation were shown to be sensitive to the voltage reduction mode. It allows to control the resulting structure of CLC droplets by adjusting the regime of electric field decrease with well-defined control parameters determining the relaxation scenario. We have carried out switching between two classes of stable states: *i)* structures with cylindrical cholesteric layers and *ii)* layer-like structures with one or more $\lambda^{+1/2}$-disclinations (Table 1). We demonstrated that the desired structure of a cholesteric droplet can be achieved using this electric field control algorithm. The reproducibility of the stable and metastable states is an important feature of the described technique. Thus, creating a liquid crystal material with programmable properties of CLC droplets becomes feasible and very promising for many applications requiring multi-stable electro-optical materials.

The proposed approach to seek for various states of CLC droplets and switch between them can be suitable for systems with a different cholesteric pitch and/or boundary conditions as well. Using cholesteric LC with a different helix pitch will require an adjustment of the control parameters (the amplitude and the step reduction of the applied voltage), which determine the scenario of transitions in CLC droplets (Fig. 4). An example of LC system with a different surface anchoring type is cholesteric droplets with tangential boundary conditions. They are known for plenty of meta-stable structures [22] and can be examined in the same way.

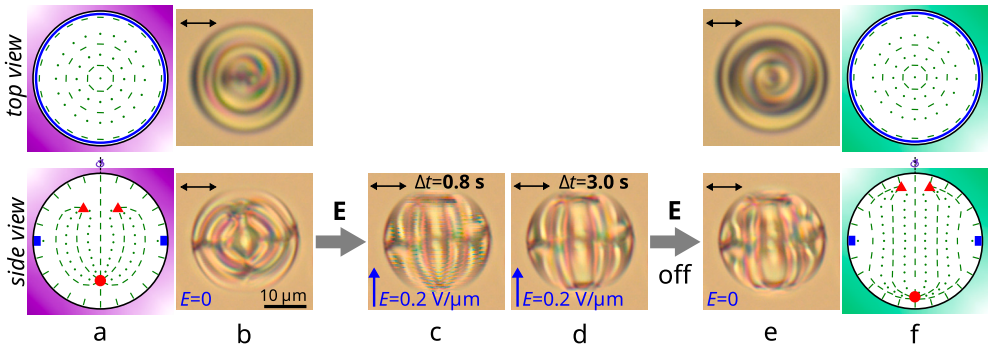

Fig. 7. Schemes of the director configuration in the cross-sections of the structure with two enclosed cholesteric layers (a). POM photos of this unstable CLC droplet with two closed cholesteric layers at $N_0 = 9.5$ (bottom row photos are taken from Supplementary Movie 8) taken before (b) and in $\Delta t = 0.8$ s (c), $\Delta t = 3.0$ s (d) after switching on the electric field $E = 0.2$ V/μm and after following switching off the voltage (e). Schemes of the stable director configuration in the cross-sections of the structure with two cylindrical cholesteric layers (f). The electric field was applied perpendicular (top row) and parallel (bottom row) to the PDLC film. The cross-sections of bulk ring defect are indicated by the red triangles, and the bulk point defect with $|m| = 2$ is shown by the red circle. The surface circular defect is indicated by the blue ring.

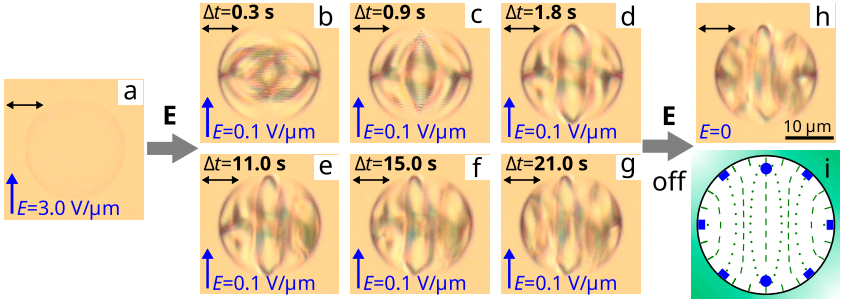

Fig. 8. POM photos of CLC droplet at $N_0 = 7.9$ (taken from Supplementary Movie 9) under the action of an electric field $E = 3.0$ V/μm (a), in $\Delta t = 0.3$ s (b), 0.9 s (c), 1.8 s (d), 11.0 s (e), 15.0 s (f), and 21.0 s (g) after an abrupt decrease in the electric field to $E = 0.1$ V/μm. POM photos of the CLC droplet after the voltage are turned-off (h) and the corresponding scheme of the director configuration in the equatorial cross-section of the droplet (i). The bulk point defects with $m = 1$ are shown by the blue circles. The applied electric field is parallel to the PDLC film plane.

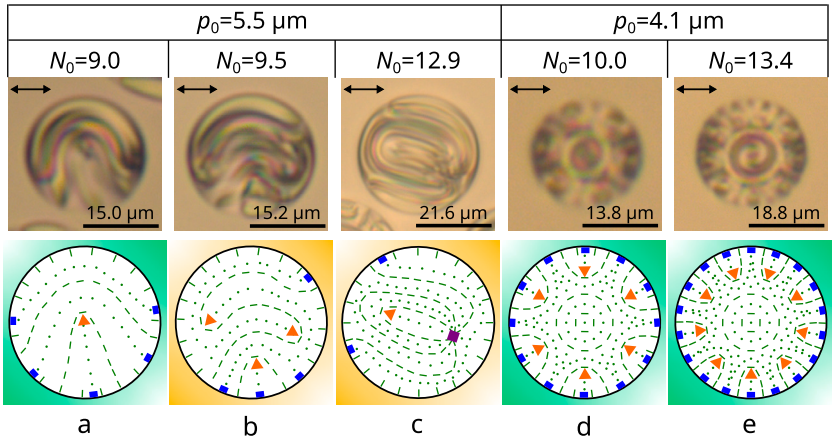

Fig. 9. POM photos of the CLC droplets (top row) and the corresponding schemes of the director configuration in the equatorial cross-section of the droplets (bottom row) after switching off the voltage. The connection of cholesteric layers in scheme (c) is shown by the purple square. The intrinsic helix pitch is $p_0 = 5.5$ μm and the value of $N_0 = 9.0$ (a), $N_0 = 9.5$ (b), $N_0 = 12.9$ (c); $p_0 = 4.1$ μm and $N_0 = 10.0$ (d), $N_0 = 13.4$ (e). The electric field was applied perpendicular to the PDLC film.

Table 1
Type of the formed stable structures depending on voltage-off mode and N_0 value.

N_0 values	Step-wise decrease in voltage	One-stage abruptly turning-off voltage	Two-stage abruptly turning-off voltage
6.0 – 8.0	layer-like structure with single $\lambda^{+1/2}$ disclination	layer-like structure with single $\lambda^{+1/2}$ disclination	structure with single cylindrical cholesteric layer
8.0 – 10.0	layer-like structure with one or two $\lambda^{+1/2}$ disclinations	layer-like structure with one or two $\lambda^{+1/2}$ disclinations	structure with two cylindrical cholesteric layers
> 10.0	layer-like structure with one or two $\lambda^{+1/2}$ disclinations	layer-like structure with one or two $\lambda^{+1/2}$ disclinations	combined structure with two cilindrical cholesteric layers

CRediT authorship contribution statement

Mikhail N. Krakhalev: Conceptualization, Investigation, Validation, Visualization, Writing – original draft. **Anna P. Gardymova:** Investigation, Methodology, Validation, Visualization, Writing – review & editing. **Vladimir Yu. Rudyak:** Conceptualization, Formal analysis, Writing – review & editing. **Vadim A. Barbashov:** Formal analysis, Visualization, Writing – review & editing. **Victor Ya. Zyryanov:** Supervision, Writing – review & editing.

Declaration of competing interest

The authors declare that they have no known competing financial interests or personal relationships that could have appeared to influence the work reported in this paper.

Data availability

Data will be made available on request.

Acknowledgements

This research was funded by Russian Science Foundation, Grant No. 20-72-10038. The research was carried out using the equipment of the shared research facilities of HPC computing resources at Lomonosov Moscow State University.

Appendix A. Supplementary material

Supplementary material related to this article can be found online at https://doi.org/10.1016/j.molliq.2023.122379.

References

[1] P. Oswald, P. Pieranski, Nematic and Cholesteric Liquid Crystals: Concepts and Physical Properties Illustrated by Experiments, The Liquid Crystals Book Series, Taylor & Francis, Boca Raton, 2005.
[2] H.-S. Kitzerow, C.B. Bahr (Eds.), Chirality in Liquid Crystals, 1st edition, Partially Ordered Systems, Springer, New York, NY, 2001.
[3] P. Shibaev, V. Kopp, A. Genack, Photonic materials based on mixtures of cholesteric liquid crystals with polymers, J. Phys. Chem. B 107 (29) (2003) 6961–6964.
[4] M. Humar, I. Muševič, 3d microlasers from self-assembled cholesteric liquid-crystal microdroplets, Opt. Express 18 (26) (2010) 26995–27003.
[5] C. Wang, C. Gong, Y. Zhang, Z. Qiao, Z. Yuan, Y. Gong, G.-E. Chang, W.-C. Tu, Y.-C. Chen, Programmable rainbow-colored optofluidic fiber laser encoded with topologically structured chiral droplets, ACS Nano 15 (7) (2021) 11126–11136.
[6] Y. Iwai, R. Iijima, K. Yamamoto, T. Akita, Y. Uchida, N. Nishiyama, Shrinkage of cholesteric liquid crystalline microcapsule as omnidirectional cavity to suppress optical loss, Adv. Opt. Mater. 8 (6) (2020) 1901363.
[7] Y. Zhang, Z. Yuan, Z. Qiao, D. Barshilia, W. Wang, G.-E. Chang, Y.-C. Chen, Tunable microlasers modulated by intracavity spherical confinement with chiral liquid crystal, Adv. Opt. Mater. (2020) 1902184.
[8] H.-S. Kitzerow, P. Crooker, G. Heppke, Chromaticity of polymer-dispersed cholesteric liquid crystals, Liq. Cryst. 12 (1) (1992) 49–58.
[9] C. Yang, B. Wu, J. Ruan, P. Zhao, L. Chen, D. Chen, F. Ye, 3d-printed biomimetic systems with synergetic color and shape responses based on oblate cholesteric liquid crystal droplets, Adv. Mater. 33 (10) (2021) 2006361.
[10] S. Mani, S. Patwardhan, S. Hadkar, K. Mishra, P. Sarawade, Effect of polymer concentration on optical and electrical properties of liquid crystals for photonic applications, Mater. Today Proc. 62 (2022) 6913–7340.
[11] G. Kocakulah, O. Koysal, Electro-optical and dielectric response of quantum dot-doped cholesteric liquid crystal composites, J. Mater. Sci., Mater. Electron. 33 (2022) 5489–5500.
[12] H.-G. Lee, S. Munir, S.-Y. Park, Cholesteric liquid crystal droplets for biosensors, ACS Appl. Mater. Interfaces 8 (39) (2016) 26407–26417.
[13] D.A. Paterson, X. Du, P. Bao, A.A. Parry, S.A. Peyman, J.A. Sandoe, S.D. Evans, D. Luo, R.J. Bushby, J.C. Jones, et al., Chiral nematic liquid crystal droplets as a basis for sensor systems, Mol. Syst. Des. Eng. 7 (2022) 607–621.
[14] G. Pirnat, M. Humar, I. Muševič, Remote and autonomous temperature measurement based on 3d liquid crystal microlasers, Opt. Express 26 (18) (2018) 22615–22625.
[15] R. Xie, N. Li, Z. Li, J. Chen, K. Li, Q. He, L.-S. Liu, S. Zhang, Liquid crystal droplet-based biosensors: promising for point-of-care testing, Biosensors 12 (2022) 758.
[16] S. Norouzi, J. Martinez-Gonzalez, M. Sadati, Chiral liquid crystal microdroplets for sensing phospholipid amphiphiles, Biosensors 12 (2022) 313.
[17] B. Gollapelli, S. Rama Raju Ganji, A. Kumar Tatipamula, J. Vallamkondu, Bio-derived chlorophyll dye doped cholesteric liquid crystal films and microdroplets for advanced anti-counterfeiting security labels, J. Mol. Liq. 363 (2022) 119952.
[18] W. Lee, S. Kumar, Unconventional Liquid Crystals and Their Applications, Walter de Gruyter GmbH & Co KG, 2021.
[19] J. Yoshioka, K. Fukao, Self-excited oscillation of the director field in cholesteric liquid crystalline droplets under a temperature gradient, J. Phys. Condens. Matter 32 (32) (2020) 325102.
[20] K. Saito, Y. Kimura, Optically driven liquid crystal droplet rotator, Sci. Rep. 12 (2022) 16623.
[21] F. Fadda, A. Lamura, A. Tiribocchi, Lattice Boltzmann modeling of cholesteric liquid crystal droplets under an oscillatory electric field, https://doi.org/10.48550/arXiv.2207.04790, 2022.
[22] D. Seč, T. Porenta, M. Ravnik, S. Žumer, Geometrical frustration of chiral ordering in cholesteric droplets, Soft Matter 8 (2012) 11982–11988.
[23] T. Orlova, S.J. Aßhoff, T. Yamaguchi, N. Katsonis, E. Brasselet, Creation and manipulation of topological states in chiral nematic microspheres, Nat. Commun. 6 (1) (2015) 7603.
[24] M.N. Krakhalev, V.Y. Rudyak, O.O. Prishchepa, A.P. Gardymova, A.V. Emelyanenko, J.-H. Liu, V.Y. Zyryanov, Orientational structures in cholesteric droplets with homeotropic surface anchoring, Soft Matter 15 (28) (2019) 5554–5561.
[25] R.L. Biagio, R.T. Souza, L.R. Evangelista, R.S. Zola, Frustrated structures and pattern formation after thermal quenches in cholesteric liquid crystal droplets, J. Mater. Chem. C 9 (27) (2021) 8623–8639.
[26] G. Posnjak, S. Čopar, I. Muševič, Points, skyrmions and torons in chiral nematic droplets, Sci. Rep. 6 (1) (2016) 26361.
[27] G. Posnjak, S. Čopar, I. Muševič, Hidden topological constellations and polyvalent charges in chiral nematic droplets, Nat. Commun. 8 (1) (2017) 14594.
[28] A.P. Gardymova, M.N. Krakhalev, V.Y. Zyryanov, A.A. Gruzdenko, A.A. Alekseev, V.Y. Rudyak, Polymer dispersed cholesteric liquid crystals with a toroidal director configuration under an electric field, Polymers 13 (5) (2021) 732.
[29] A. Gardymova, V.Y. Zyryanov, V. Loiko, Multistability in polymer-dispersed cholesteric liquid crystal film doped with ionic surfactant, Tech. Phys. Lett. 37 (9) (2011) 805–808.
[30] A.P. Gardymova, M.N. Krakhalev, V.Y. Rudyak, V.A. Barbashov, V.Y. Zyryanov, Polymer-dispersed cholesteric liquid crystal under homeotropic anchoring: electrically induced structures with $\lambda^{1/2}$-disclination, Polymers 14 (7) (2022) 1454.
[31] D. Seč, S. Čopar, S. Žumer, Topological zoo of free-standing knots in confined chiral nematic fluids, Nat. Commun. 5 (1) (2014) 3057.
[32] V.Y. Rudyak, M.N. Krakhalev, A.P. Gardymova, A.S. Abdullaev, A.A. Alekseev, V.Y. Zyryanov, Effect of elastic constants on electrically induced transition in twisted radial cholesteric droplets, Sci. Rep. 12 (1) (2022) 9565.
[33] M.N. Krakhalev, A.P. Gardymova, O.O. Prishchepa, V.Y. Rudyak, A.V. Emelyanenko, J.-H. Liu, V.Y. Zyryanov, Bipolar configuration with twisted loop defect in chiral nematic droplets under homeotropic surface anchoring, Sci. Rep. 7 (1) (2017) 14582.
[34] H.-S. Kitzerow, Polymer-dispersed liquid crystals from the nematic curvilinear aligned phase to ferroelectric films, Liq. Cryst. 16 (1) (1994) 1–31.
[35] O. Prishchepa, M. Krakhalev, V. Rudyak, V. Sutormin, V. Zyryanov, Electrically turning periodic structures in cholesteric layer with conical–planar boundary conditions, Sci. Rep. 11 (1) (2021) 8409.
[36] Y. Geng, J. Noh, I. Drevensek-Olenik, R. Rupp, G. Lenzini, J.P.F. Lagerwall, High-fidelity spherical cholesteric liquid crystal Bragg reflectors generating unclonable patterns for secure authentication, Sci. Rep. 6 (1) (2016) 26840.
[37] M.N. Krakhalev, A.P. Gardymova, A.V. Emel'yanenko, J.-H. Liu, V.Y. Zyryanov, Untwisting of the helical structure of cholesteric droplets with homeotropic surface anchoring, JETP Lett. 105 (1) (2017) 51–54.